Optical Materials 37 (2014) 93–96

Contents lists available at ScienceDirect

Optical Materials

journal homepage: www.elsevier.com/locate/optmat

Continuous-wave lasing at 1.06 μm in femtosecond laser written Nd:KGW waveguides

Hongliang Liu [a], Qiang An [a], Feng Chen [a,*], Javier R. Vázquez de Aldana [b], Blanca del Rosal Rabes [c]

[a] School of Physics, State Key Laboratory of Crystal Materials and Key Laboratory of Particle Physics and Particle Irradiation (MOE), Shandong University, Jinan 250100, China
[b] Laser Microprocessing Group, Universidad de Salamanca, Salamanca 37008, Spain
[c] Fluorescence Imaging Group, Departamento de Física de Materiales, Facultad de Ciencias, Universidad Autónoma de Madrid, Madrid 28049, Spain

ARTICLE INFO

Article history:
Received 8 April 2014
Received in revised form 2 May 2014
Accepted 5 May 2014
Available online 29 May 2014

Keywords:
Waveguide lasers
Femtosecond laser writing
Optical waveguides
Nd:KGW crystal

ABSTRACT

We report on the buried channel waveguide laser at 1065 nm in Nd:KGW waveguides fabricated by femtosecond laser writing with dual-line approach. A relatively high scanning speed of 0.5 mm/s enables acceptable propagation loss less than 2 dB/cm. The fluorescence emission spectra of Nd^{3+} ions measured shows that the fluorescence properties were well preserved in the waveguide region. A stable continuous wave laser at 1065 nm has been obtained at room temperature in the buried channel waveguides by optical pumping at 808 nm. A maximum output power of 33 mW and a slope efficiency of 52.3% were achieved in the Nd:KGW waveguide laser system.

1. Introduction

Waveguide lasers based on active media are the minor light sources that play an important role in the integrated photonics and telecommunication systems [1]. Owing to the confinement of the light field within compact volumes, the light in optical waveguides can reach relatively high optical intensities; consequently, laser oscillations in active gain waveguides may possess low lasing thresholds and comparable efficiency with respect to those of the bulk lasers [2–4]. Compared with one-dimensional (1D) (planar or slab waveguides), the two-dimensional (2D) (in channel or ridge configurations) waveguides can confine the light propagation in 2Ds, reaching higher optical density, and can possibly applied to construct waveguides are possible applied to construct waveguide platforms and achieve multiple functions [5]. There are many techniques for fabricating 2D waveguides in optical materials reported before, such as proton beam writing [6], ion exchange [7], ion implantation combined with masking technique [8] and femtosecond laser (fs-laser) writing [9–28]. Since the pioneering work of Davis et al. in 1996 [9], the fs laser writing has become a powerful technique for three-dimensional volume microstructuring of dielectric materials [10–15]. The energy of the focused laser is absorbed through nonlinear process such as two-photon or multiphoton absorption, inducing lattice stress, defect creation and heat accumulation in a very short time [13–15]. Because of this special feature, focused fs-laser pulses produce stress-induced effect and lattice damage on a micro- or submicro-scale in the focal volume inside the material, in which stable refractive-index changes may be created [15,16]. In recent years, active waveguides in different crystals and glasses have been produced by fs laser writing through stress-induced mechanisms that have been generated in some of these samples, such as Nd doped YAG or GGG, Yb:YAG, Nd doped YVO_4 or $GdVO_4$ and Yb doped KGW or KYW [14–20]. The dual-line configuration, which is so-called Type II waveguide, is popular in crystalline materials, typically with a stress-induced guiding region between the two tracks of negative index changes [17,19–24]. The Type II stress-induced waveguides exhibit low-order-mode features, and possess high thermal stabilities.

Neodymium-doped potassium gadolinium tungstate (Nd:KGd$(WO_4)_2$ or Nd:KGW) is widely known as an effective laser gain material for Raman laser due to the attractive features of this crystal, such as high third-order nonlinear susceptibility, high thermal conductivity and low lasing threshold with a broad and strong absorption band [24–26]. The fabrication of dual-line waveguides in Nd:KGW crystal has been realized, however, no lasing performance has been reported [27,28]. In this work, we utilized Nd:KGW channel waveguides with different separation between the two track lines, investigating the near-infrared lasing properties of the waveguides.

* Corresponding author. Tel.: +86 531 88363007; fax: +86 531 88363350.
E-mail address: drfchen@sdu.edu.cn (F. Chen).

http://dx.doi.org/10.1016/j.optmat.2014.05.005
0925-3467/

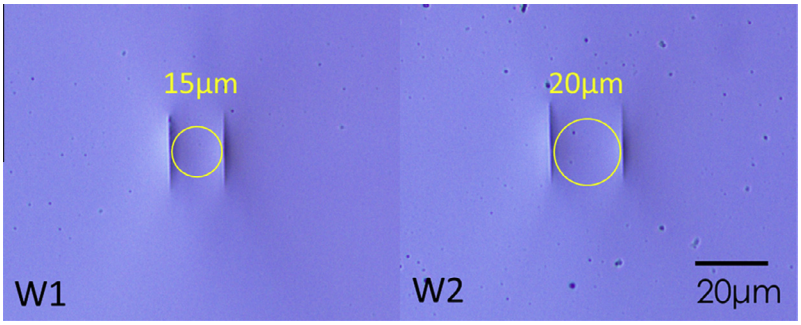

Fig. 1. Optical cross-sectional image (under transmission mode) of the channel waveguides in Nd:KGW fabricated by fs laser writing. Separation of the W1 and W2 are 15 μm and 20 μm, respectively.

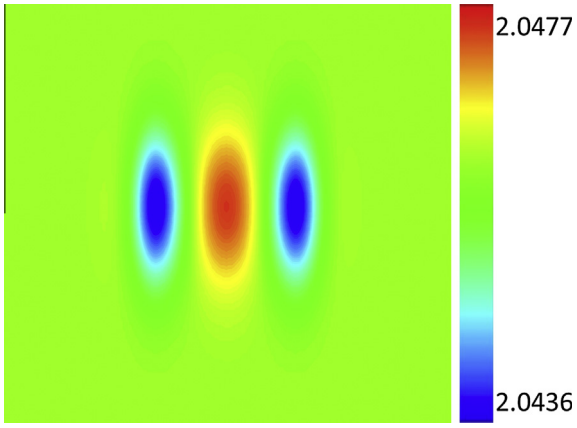

Fig. 2. Distribution modeled of the refractive index (n_q) at the cross section of the Nd:KGW channel waveguide (W1).

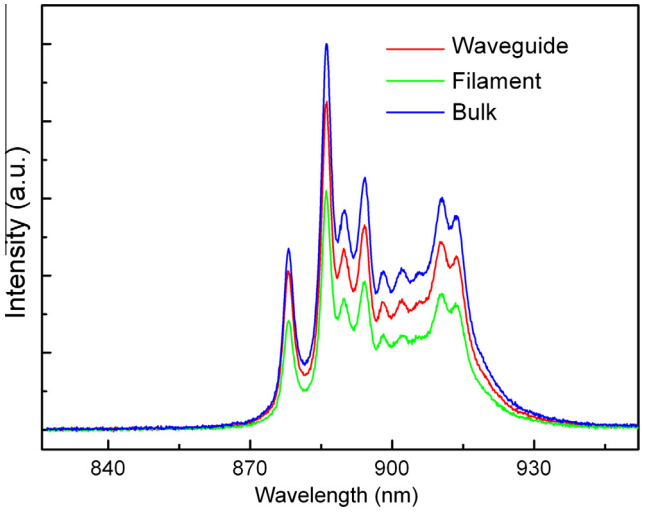

Fig. 3. Comparison of the micro-photoluminescence spectra corresponding to Nd^{3+} ions at $^4F_{3/2} \rightarrow {}^4I_{9/2}$ transition obtained after 488 nm excitation at the waveguide (red line), filament (green line) and bulk area (blue line) at room temperature. (For interpretation of the references to colour in this figure legend, the reader is referred to the web version of this article.)

2. Experiments in details

The *m*-cut Nd:KGW (doped with 1 at.% Nd^{3+} ions) crystal was cut to $8(p) \times 8(q) \times 2(m)\,mm^3$ and optical polished. The buried channel waveguides were fabricated by fs laser writing, using the facilities at University de Salamanca, Spain. A Ti:sapphire laser system (Spitfire, Spectra Physics, USA) delivered a linearly polarized laser with a repetition rate of 1 kHz and a temporal duration of 120 fs, inscribed the "dual-line" configuration waveguide. The laser beam at a central wavelength of 796 nm (spectral width: 9 nm) was focused by a 20× objective lens at a location of 150 μm beneath the surface of the sample. The pulse energy incident on sample was set to 0.42 μJ by using a calibrated neutral density filter, and a half-wave plate and a linear polarizer. Then the channel waveguides (W1 and W2) were fabricated by the laser beam scanning at a velocity of 500 μm/s on a *XYZ* motorized stage with separations of 15 μm and 20 μm. The propagation losses of the waveguides W1 and W2 are less than 2.4 dB/cm and 2 dB/cm measured under 632.8 nm with the Fabry–Perot resource method [29].

In order to study the fluorescence properties of Nd^{3+} ions in the waveguide cross section as well as to evaluate the potential applications of the fs-laser inscribed dual-line waveguides as laser gain medium, a fiber-coupled confocal microscope was utilized to measure the μ-PL at the Universidad Autónoma de Madrid, Spain (Olympus BX-41). A 488 nm continuous wave (cw) diode laser was provided for the optical excitation, which is focused into the sample by using a 50× microscope objective with a N.A. of 0.55. The radius of the 488 nm spot formed at the sample's surface was estimated to be ~0.53 μm. The subsequent backscattered radiation signal (μ-PL) generated by Nd^{3+} ions was collected with the same microscope objective and, after passing through a set of filters, lenses and confocal apertures (with diameter ~25 μm of the confocal pinhole), it was spectrally analyzed by a high resolution spectrometer (iHR320 Horiba Jobin Yvon). The sample was mounted on a three dimensional motorized stage with a spatial resolution better than 10 nm.

The laser experiments were performed under a typical end-pumped arrangement as reported before. A tunable Ti:sapphire laser (Coherent MBR 110) launched a cw 808 nm linearly polarized pump beam, as the pump beam, which was coupled into the waveguide by using a convex lens (with focal length of 25 mm). Two dielectric mirrors (the input one with reflectivity >99% at 1060–1065 nm and 98% transmission at 800–810 nm, and the output one with reflectivity >95% at 800–810 nm and ~60% transmission at 1000–1100 nm) were adhered to the two end faces to construct a Fabry–Perot oscillating cavity. The output coupler of the waveguide laser system was then determined to be 60%. The length of the laser cavity was 8 mm. We used a 20× microscope objective to collect the output lasers from the waveguide's exit facet after a filter with high reflectivity at 790–810 nm and an IR CCD to image the generated laser radiation at IR wavelength, while a spectrometer and a powermeter were used to characterize the spectrum and output power.

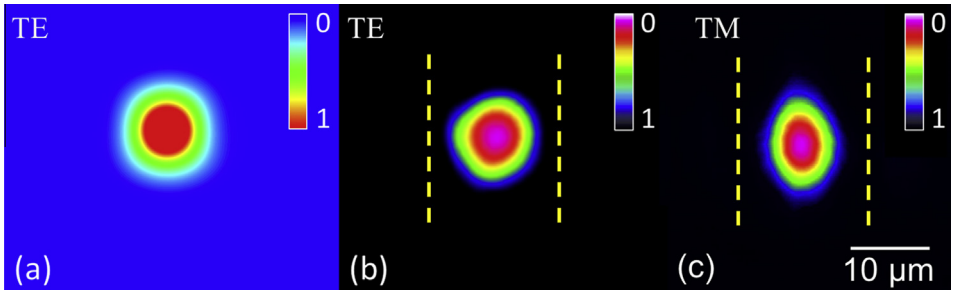

Fig. 4. (a) Calculated TE modal profile of the waveguide W1 at 632.8 nm, (b) and (c) are measured near-field intensity distribution of the channel waveguide (W1) at TE and TM mode. The dashed lines stand for the fs-laser inscription tracks.

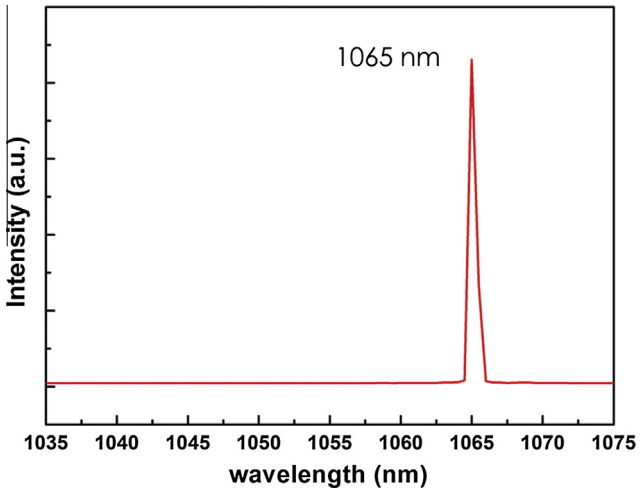

Fig. 5. The cw laser oscillation spectrum obtained from Nd:KGW channel waveguides with optical pumping at 808 nm at room temperature. The peak position stays at 1065 nm and the FWHM is about 0.4 nm.

3. Results and discussion

Fig. 1 depicts the optical transmission microscope photograph of the channel waveguides in Nd:KGW crystal. The separations of the two filaments (the tracks of the fs laser writing) are 15 μm and 20 μm, respectively. The Type II channel waveguides were located at the central area between the two damage tracks.

It is impossible to use the m-line technique to measure the change of the refractive index as the channel waveguides were located 150 μm beneath the boundary of crystal. We reconstructed 2D refractive index (n_q) profile of the channel waveguide W1 as shown in Fig. 2 based on the assumption of the distribution being a step-like one and the measurement of N.A. of the waveguide. We obtained an approximately maximum value of the refractive index change in the waveguide region by using the formula

$$\Delta n = \frac{\sin^2 \Theta_m}{2n} \tag{1}$$

where n is the refractive index of the bulk material, the Θ_m is the maximum incident angle at which the transmitted power is occurring without any change [30]. As one can see, there is a positive refractive index change $\Delta n_w = 1.2 \times 10^{-3}$ in the waveguide core and a negative refractive index change $\Delta n_f = -2.9 \times 10^{-3}$ in the filaments due to the induced stress and lattice damage which will cause a micro-modification to the unit cell volume [31].

To illustrate the influence of fs-laser micromachining process on the fluorescence properties of Nd^{3+} ions, we measured the micro-photoluminescence spectra corresponding to the transition $^4F_{3/2} \rightarrow {}^4I_{9/2}$ of Nd^{3+} ions after 488 nm excitation at the waveguide which is displayed in Fig. 3.

With an overall spatial resolution better than 10 nm and the horizontal width of the filaments being 600–700 nm, we obtained the confocal μPL emission spectra from a non-processed area (bulk), the center of the channel waveguide (WG1) and the track of the fs-laser inscription. With the comparison of the emission spectra, we found that the intensity of the emitted fluorescence

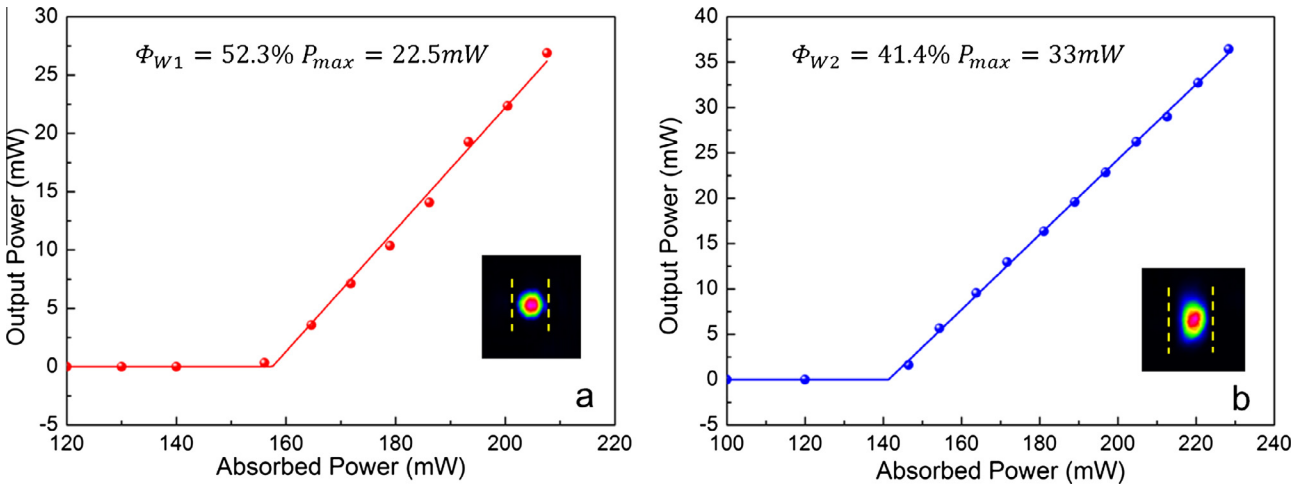

Fig. 6. The cw waveguide laser (along TE polarization) output power as a function of the absorbed pump power at 808 nm collected from waveguides (a) W1 and (b) W2, respectively. The inset graphs show the intensity distributions of the output light from each waveguide at 1065 nm.

signals in the center of the waveguide reaches 85% of the values of the bulk area, while that in the filament region decreases down to only 65%. This obvious contrast means that the original PL features have not been deteriorated in the fs-laser inscription process, and well preserved PL properties suggests potential applications of the fs-laser micromachining Nd:KGW system for laser generation.

Fig. 4(a) displays the calculated TE (q polarization) mode profile of the waveguide (W1) with a separation of 15 μm at 632.8 nm. The propagation of the light in the waveguide was simulated by the finite-difference beam propagation method (FD-BPM) based on the reconstructed refractive index distribution. The measured TE and TM (m polarization) mode near-field intensity distribution of the channel waveguide (W1) is displayed in Fig. 4(b) and (c). Fig. 5(a) and (b) shows quasi-circular distribution of the profile at TE mode with high symmetry, which is much better than the TM mode displayed in Fig. 4(c). In addition, the comparison between Fig. 4(b) and the calculated mode in Fig. 4(a) shows that the experimental result is in good agreement with the expected one, which demonstrates the accuracy and reasonability of the reconstructed distribution of the refractive index in the waveguide region shown in Fig. 2.

The measured emission spectrum around 1065 nm from the Nd:KGW channel waveguide as obtained when pumping well above threshold is shown in Fig. 5. The FWHM of the laser spectrum is about 0.4 nm. The emission line with peak position at 1065 nm clearly observed denotes a laser oscillation line, which is relevant to the $^4F_{3/2} \rightarrow {}^4I_{11/2}$ fluorescence band of Nd^{3+} ions.

We measured the laser performance of the W1 and W2 waveguides with pumping at 808 nm by a typical end-face coupling experiment at room temperature. All the experimental results for channel waveguides were recorded under their respective optimized conditions by using the same pumping system. Fig. 6(a) illustrates the cw waveguide (TE mode) laser output power as a function of the absorbed power at 808 nm collected from waveguide W1. According to a linear fitting of the data, the maximum output power ($P_{max,W1}$) is 22.5 mW with slope efficiency Φ_{W1} being 52.3% as shown in Fig. 6(b). Meanwhile, the maximum output power ($P_{max,W2}$) is 33 mW and the slope efficiency Φ_{W2} is 41.4% calculated from the data of the waveguide W2 in Nd:KGW. The thresholds of the waveguides are 157 mW and 141 mW, respectively. The larger separation of the two filaments in waveguide W2 lead to a higher optical conversion efficiency (η_{W2} = 14.3%) compared with that of waveguide W1 (η_{W1} = 11%) making a contribution of higher maximum output power and lower threshold. Partly due to own lower coupling efficiency and higher loss than the waveguide W2, waveguide W1 achieved a higher slope efficiency. The inset graphs show the measured single mode near-field distribution of the output laser beam at 1065 nm collected by the IR CCD camera along TE polarization, while there was no laser oscillation generated at TM polarization in the pumping experiment as a consequence of the lower absorption coefficient at this polarization.

4. Conclusion

In conclusion, we have fabricated channel waveguides by fs-laser writing in Nd:KGW. The simulated and measured highly symmetric near-field intensity distribution shows good performance of the waveguide. Stable cw laser oscillation at 1065 nm has been obtained in the buried channel waveguides pumped by laser at 808 nm at room temperature with a maximum output power of 33 mW and a propagation loss of 2 dB/cm. The highest slope efficiency about 52.3% has been achieved. The results here show a potential application of fs laser micromachining in fabricating channel waveguide in Nd:KGW crystals as cost-effective integrated laser source. Further work would be performed on the Q-switching of the waveguide system for the pulsed laser generation.

Acknowledgements

The work is supported by the National Natural Science Foundation of China (No. 11274203), the Specialized Research Fund for the Doctoral Program of Higher Education of China (No. 20130131130001) and Junta de Castilla y León under project SA086A12-2. Support from the Centro de Láseres Pulsados (CLPU) is also acknowledged.

References

[1] C. Grivas, Prog. Quantum Electron. 35 (2011) 159–239.
[2] J.I. Mackenzie, IEEE J. Sel. Top. Quantum Electron. 13 (2007) 626–637.
[3] E. Cantelar, D. Jaque, G. Lifante, Opt. Mater. 34 (2012) 555–571.
[4] C. Grivas, C. Corbari, G. Brambilla, P.G. Lagoudakis, Opt. Lett. 37 (2012) 4630–4632.
[5] F. Chen, Crit. Rev. Solid State Mater. Sci. 33 (2008) 165–182.
[6] F. Watt, M.B.H. Breese, A.A. Bettiol, J.A. van Kan, Mater. Today 10 (2007) 20–29.
[7] E.M. Rodríguez, D. Jaque, E. Cantelar, F. Cussó, G. Lifante, A.C. Busacca, A. Cino, S.R. Sanseverino, Opt. Express 15 (2007) 8805–8811.
[8] F. Chen, Laser Photonics Rev. 6 (2012) 622–640.
[9] K.M. Davis, K. Miura, N. Sugimoto, K. Hirao, Opt. Lett. 21 (1996) 1729–1731.
[10] R.R. Gattass, E. Mazur, Nat. Photonics 2 (2008) 219–225.
[11] J. Burghoff, S. Nolte, A. Tünnermann, Appl. Phys. A 89 (2007) 127–132.
[12] M. Ams, G.D. Marshall, P. Dekker, J. Piper, M. Withford, Laser Photonics Rev. 3 (2009) 535–544.
[13] F. Vega, J. Armengol, V. Diez-Blanco, J. Siegel, J. Solis, B. Barcones, A. Perez-Rodriguez, L. Loza-Alvarez, Appl. Phys. Lett. 87 (2005) 021109.
[14] A. Ródenas, J.A. Sanz García, D. Jaque, G.A. Torchia, C. Méndez, I. Arias, L. Roso, F. Agulló-Rueda, J. Appl. Phys. 100 (2006) 033521.
[15] F. Chen, J.R. Vázquez de Aldana, Laser Photonics Rev. 8 (2014) 250–275.
[16] A. Ródenas, G.A. Torchia, G. Lifante, E. Cantelar, J. Lamela, F. Jaque, L. Roso, D. Jaque, Appl. Phys. B 95 (2009) 85–96.
[17] Y. Tan, A. Rodenas, F. Chen, R.R. Thomson, A.K. Kar, D. Jaque, Q.M. Lu, Opt. Express 18 (2010) 24994–24999.
[18] R. Mary, S.J. Beecher, G. Brown, R.R. Thomson, D. Jaque, S. Ohara, A.K. Kar, Opt. Lett. 37 (2012) 1691–1693.
[19] J. Siebenmorgen, T. Calmano, K. Petermann, G. Huber, Opt. Express 18 (2010) 16035–16040.
[20] Y. Tan, F. Chen, J.R. Vázquez de Aldana, G.A. Torchia, A. Benayas, D. Jaque, Appl. Phys. Lett. 97 (2010) 0311191.
[21] J.R. Macdonald, R.R. Thomson, S.J. Beecher, N.D. Psaila, H.T. Bookey, A.K. Kar, Opt. Lett. 35 (2010) 4036–4038.
[22] T. Sabapathy, A. Ayiriveetil, A.K. Kar, S. Asokan, S.J. Beecher, Opt. Mater. Express 2 (2012) 1556–1561.
[23] G.A. Torchia, A. Rodenas, A. Benayas, E. Cantelar, L. Roso, D. Jaque, Appl. Phys. Lett. 92 (2008) 111103.
[24] F.M. Bain, A.A. Lagatsky, R.R. Thomson, N.D. Psaila, N.V. Kuleshov, A.K. Kar, W. Sibbett, C.T.A. Brown, Opt. Express 17 (2009) 22417–22422.
[25] C.J. Flood, D.R. Walker, H.M. van Driel, Appl. Phys. B 60 (1995) 309–312.
[26] P.A. Loiko, K.V. Yumashev, N.V. Kuleshov, V.G. Savitski, S. Calvez, D. Burns, A.A. Pavlyuk, Opt. Express 17 (2009) 23536–23543.
[27] S.M. Eaton, C.A. Merchant, R. Iyer, A.J. Zilkie, A.S. Helmy, Appl. Phys. Lett. 92 (2008). 0811051–0811053.
[28] X. Liu, S. Qu, Y. Tan, C. Zhang, F. Chen, Appl. Phys. B 103 (2011) 145–149.
[29] R. Ramponi, R. Osellame, M. Marangoni, Rev. Sci. Instrum. 73 (2002) 1117–1120.
[30] J. Siebenmorgen, K. Petermann, G. Huber, K. Rademaker, S. Nolte, A. Tunnermann, Appl. Phys. B 97 (2009) 251–255.
[31] G.A. Torchia, P.F. Meilán, A. Rodenas, D. Jaque, C. Mendez, L. Roso, Opt. Express 15 (2007) 13266–13271.